ASSOCIATIE EURATOM-FOM

FOM-INSTITUUT VOOR PLASMAFYSICA

RIJNHUIZEN – NIEUWEGEIN – NEDERLAND

EQUILIBRIUM AND STABILITY ASPECTS OF A SCREW-PINCH BASED ON THE SHARP-BOUNDARY MODEL OF A HIGH-BETA TOKAMAK

by

J. Rem

Rijnhuizen Report 81-130

ASSOCIATIE EURATOM-FOM

FOM-INSTITUUT VOOR PLASMAFYSICA

RIJNHUIZEN – NIEUWEGEIN – NEDERLAND

February 1981

EQUILIBRIUM AND STABILITY ASPECTS OF A SCREW-PINCH BASED ON THE SHARP-BOUNDARY MODEL OF A HIGH-BETA TOKAMAK

by

J. Rem

Rijnhuizen Report 81-130

This work was performed as part of the research programme of the association agreement of Euratom and the "Stichting voor Fundamenteel Onderzoek der Materie" (FOM) with financial support from the "Nederlandse Organisatie voor Zuiver-Wetenschappelijk Onderzoek" (ZWO) and Euratom.

C O N T E N T S

		page
	ABSTRACT	1
1.	INTRODUCTION	2
2.	THE EQUILIBRIUM OF THE SHARP-BOUNDARY MODEL OF A HIGH-BETA TOKAMAK WITH FORCE-FREE CURRENTS	4
3.	SOLUTION TO THE ILL-POSED PROBLEM	9
4.	FLUX SURFACES OUTSIDE A CIRCULAR, ELLIPTICAL AND A D-SHAPED CROSS-SECTION	14
5.	THE STABILITY OF THE SCREW-PINCH	23
6.	CONCLUSIONS	26
	REFERENCES	28
	APPENDIX A Skin current model versus diffuse plasma currents	29
	APPENDIX B Fixed-boundary versus free-boundary analysis	33
	TABLES	35
	FIGURES	37

EQUILIBRIUM AND STABILITY ASPECTS OF A SCREW-PINCH BASED ON THE SHARP-BOUNDARY MODEL OF A HIGH-BETA TOKAMAK

by

J. Rem
Association Euratom-FOM
FOM-Instituut voor Plasmafysica
Rijnhuizen, Nieuwegein, The Netherlands

ABSTRACT

The sharp-boundary model of a high-beta tokamak surrounded by force-free currents (FFC) should yield a good description of the magnetohydrodynamic stability of a screw-pinch: a tokamak with uniform q-profile. To arrive at the relationship between the equilibrium parameters giving rise to such a q-profile in the FFC region the poloidal field outside the plasma (with a prescribed cross-section) must be determined. An analytical solution has been derived for this field from which the desired relationship can be obtained by numerical means. From the results of a number of cross-sections it is evident that an approximation can be made that leads to this relationship more readily. Based on the latter the stability of a screw-pinch with a number of different cross-sections has been analyzed.

1. INTRODUCTION

The stability analysis of a toroidal sharp-boundary, high-beta tokamak plasma [1] surrounded by force-free currents is much simpler than that of a diffuse plasma because it involves relatively few parameters. It was exactly this feature that made the study of this model so attractive for it permitted a complete scan of the parameter space. Apart from its dependence on the equilibrium parameters: beta, the safety factor q on the plasma surface S, and the strength of the force-free currents (FFC), the stability depends only on the poloidal field on S. In other words the equilibrium fields outside the plasma do not enter the stability problem. Of course these fields are in principle fully determined by the equilibrium parameters.

The screw-pinch "Spica" [2] has been so designed that optimal use is made of FFC. The experiment is axisymmetric and the plasma is created in a quartz vacuum vessel. This vessel is surrounded by a thick copper shell into which toroidal and poloidal field components are fed at equal rates during the formation phase of the plasma. In the low density region behind the shock this process gives rise to large FFC and an almost uniform q-profile. A crowbar system effectively closes the shell for the poloidal field so that a plasma - surrounded by FFC - is confined whereby the outermost magnetic surface coincides with the copper shell. The result is that the FFC affect both the equilibrium and the stability. The effect on the first one lies in its effect on the shape of the plasma cross-section S and the position of S with respect to the copper shell. Its effect on stability lies mainly in the contribution of the FFC region to the potential energy of a perturbation (δW).

The sharp-boundary high-beta tokamak with FFC should yield a good description of the stability of the screw-pinch in which plasmas with high betas are confined. However, in the stability analysis the shape of the plasma cross-section is assumed and the equilibrium parameters are independent. This is not true in the screw-pinch because the manner of creation leads to a uniform q-profile. Consequently, to apply the high-beta tokamak results to the screw-pinch we must determine which combination of equilibrium parameters yields such a q-profile. To answer this question it is necessary to determine the fields in the force-free field region surrounding the plasma of which the cross-section is given. In this paper we show that in the high-beta tokamak ordering this problem can be solved by analytic means. However, to obtain from these fields the desired relationship between the equilibrium parameters that give rise to a screw-pinch is cumbersome. Fortunately, a good approximation to this has been found that consists of a simple integral condition involving the field on the plasma surface only.

The analysis of the equilibrium of the sharp-boundary model of a high-beta tokamak (Section 2) shows that the poloidal magnetic field in the FFC region is described by a flux function that must satisfy a simple Poisson equation in the plane of the cross-section. However, due to the manner in which the problem is posed: determine the equilibrium fields outside a given plasma surface, this problem is ill-posed. In other words, the elliptic problem has the wrong boundary conditions: they are Cauchy boundary conditions. In the following section (Section 3) it is shown how the method developed in Ref. 3 for the case of a vacuum region can be extended to include a region with FFC. The method consists essentially of an analytic continuation of the boundary data on S and results in an analytic expression for the poloidal field in the FFC region. In section 4 this solution is employed to evaluate the fields in the FFC region for a number of specific cross-sections: the circle, the ellipse, and the D-shape.

Based on the results of section 4 we conclude that, as far as the equilibrium parameters are concerned, the screw-pinch mode can well be found from the simple condition on the safety factor q on S: $dq/d\psi = 0$. For any cross-section given in a parametric form this condition leads to a simple integral condition on the poloidal field from which the relationship between the equilibrium parameters corresponding to the screw-pinch mode can easily be determined. For a number of cross-sections this has been done (Section 5) and the corresponding marginal stability points indicated in the stability diagram for the high-beta tokamak with FFC.

The conclusions are presented in section 6. Here we point out that some of the properties of the fields in the FFC region can be ascribed to the sharp-boundary model of the plasma. Furthermore, a comparison between those fields, evaluated on the basis of the treatment given here, with those from a free-boundary analysis shows that the first method should be used with care.

2. THE EQUILIBRIUM OF THE SHARP-BOUNDARY MODEL OF A HIGH-BETA TOKAMAK WITH FORCE-FREE CURRENTS

In the sharp-boundary model of a tokamak a plasma (V^p) with a uniform pressure is confined by surface currents. The form of the model that we are interested in is characterized by force-free currents, i.e., the usual vacuum region surrounding the plasma is replaced by a region carrying force-free currents.

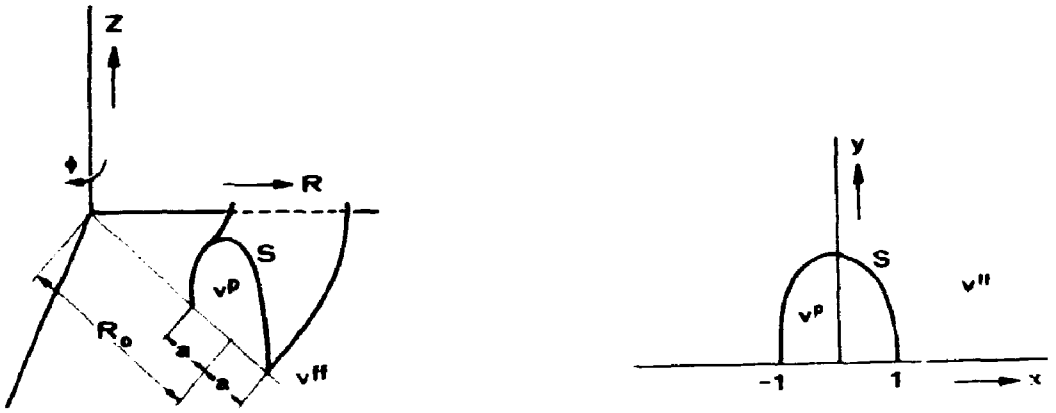

The variables describing the plasma are:

$$p = \text{constant}, \quad \rho = \text{constant}$$
$$\underline{B} = B_\phi \hat{e}_\phi = R_o B_o / R \hat{e}_\phi , \quad B_o = B_\phi(R = R_c) , \tag{1}$$

where the coordinate system (R,z,ϕ) is that shown above and R_o stands for the major radius of the plasma. The geometry of the cross-section S is given in the dimensionless coordinate system (x,y) that is centred at R_o; it is given by:

$$x_s = x_s(t) = (R - R_o)/a ,$$
$$y_s = y_s(t) = z/a . \tag{2}$$

S will be restricted to convex curves and to curves that are symmetric with respect to the x-axis; t is an angle-like variable along S that takes on values between 0 and 2π. The region V^{ff} is characterized by the presence of force-free currents and its physical variables are:

$$\hat{p} = 0 \ , \quad \hat{\rho} = 0 \ ,$$
$$\underline{\nabla} \times \underline{\hat{B}} = \alpha \underline{\hat{B}} \ , \quad \alpha = \text{constant} \ . \tag{3}$$

Like in the stability studies we restrict ourselves to a uniform α. The confinement by surface currents leads to the pressure balance relation across S:

$$p + \tfrac{1}{2} B_\phi^2 = (\hat{B}_p^2 + \hat{B}_\phi^2)/2 \ , \tag{4}$$

where hats indicate that the variables are to be taken on the force-free field side. Since S is a flux surface the poloidal variation of the toroidal fields on S is given by:

$$B_\phi / B_o = \hat{B}_\phi / \hat{B}_o = 1/\left(1 + \varepsilon x_s(t)\right) \ , \tag{5}$$

where ε refers to the inverse aspect ratio a/R_o.

The equilibrium is completely described by the above equations. Since the poloidal field $\hat{B}_p$ depends only on the plasma parameters and not on α (see Eq. 4), the force-free currents do not affect the equilibrium fields on S. Consequently, the surface current model has reduced the equilibrium problem to determining the solution of (3) with a boundary condition that is independent of α.

At this point we introduce the high-beta tokamak ordering. The various quantities are ordered as follows:

$$\begin{aligned} &B_\phi / B_o \approx \hat{B}_\phi / \hat{B}_o \sim 1 \ , \\ &\hat{B}_p / \hat{B}_o \sim \varepsilon \ , \\ &\beta \equiv 2p/B_o^2 \sim \varepsilon \ , \\ &\alpha a \sim \varepsilon \ . \end{aligned} \tag{6}$$

This ordering imposes a certain restriction on V^{ff} and α. For too large a value of α the first condition of (6) will be violated near the outer boundary of V^{ff}. Application of the ordering to (4) yields:

$$\begin{aligned} &(\hat{B}_\phi - B_\phi)/\varepsilon B_o = \beta/2\varepsilon + O(\varepsilon) \ . \\ &\hat{B}_p(t)/\varepsilon B_o = \sqrt{4\beta/(\varepsilon k^2)} \left[1 - \tfrac{1}{2} k^2 \left(1 - x_s(t)\right)\right]^{1/2} \ , \end{aligned} \tag{7}$$

where k is a free parameter of unit range ($0 \leq k \leq 1$). The first equa-

tion shows that the confinement is θ pinch-like, i.e., the pressure is balanced by the toroidal field. The parameter k can be related to the safety factor q (on S) or to the plasma current. In Ref. 1 we decided to relate it to the current and introduced another safety factor q^*:

$$q^* = a L \tilde{B}_\phi / R I_\phi = \varepsilon B_o / \langle \tilde{B}_p \rangle \ , \tag{8}$$

where L refers to the circumference of the cross-section and the average of a quantity along S is defined by:

$$\langle A \rangle = \frac{1}{L} \int d\ell \, A \ , \tag{9}$$

$d\ell$ being an infinitesimal length along S. The introduction of q^* as an equilibrium parameter instead of q not only eliminates the undesirable behaviour of the safety factor q going to infinity when the separatrix approaches the plasma surface but has the additional advantage that the stability boundary at low-beta becomes insensitive to the shape of the cross-section. Obviously, we can write down an explicit relationship between k, β and q^*. However, it is better to employ the relationship between k and the poloidal beta instead. At this point it is useful to introduce a poloidal field normalized with respect to q^*:

$$\tilde{b}_p(t) = \frac{q^* \tilde{B}_p(t)}{\varepsilon B_o} = \frac{[\,1 - \tfrac{1}{2}k^2 (1 - x_s(t))\,]^{1/2}}{\langle [\,1 - \tfrac{1}{2}k^2 (1 - x_s(t))\,]^{1/2} \rangle} \ , \tag{10}$$

so that $\langle \tilde{b}_p(t) \rangle = 1$. From (7), (8), (9) and (10) we see that the usual poloidal beta depends in a simple way on β and q^* and is directly related to k:

$$\varepsilon\beta_p \equiv \frac{2p\varepsilon}{\langle \tilde{B}_p \rangle^2} = (\beta/\varepsilon) q^{*2} = \tfrac{1}{4}k^2 / \langle [\,1 - \tfrac{1}{2}k^2 (1 - x_s(t))\,]^{1/2} \rangle^2 \ . \tag{11}$$

The meaning of the range of k is seen to be: k = 0 corresponds to small $\varepsilon\beta_p$ and in practice to a small β, while the limit k = 1 corresponds to the equilibrium limit, i.e., when the separatrix has moved onto S at $x_s = -1$,

$$\varepsilon\beta_{p,crit} = \frac{1}{2 \langle \sqrt{1 + x_s} \rangle^2} \ . \tag{12}$$

Since we are interested in the q-profile in V^{ff} we need q on S in terms of the plasma parameters. From the definition of q it is clear that the

ordering together with (10) leads to the expression:

$$q/q^* = e \langle [1 - \tfrac{1}{2}k^2 (1 - x_s(t))]^{1/2} \rangle \langle [1 - \tfrac{1}{2}k^2 (1 - x_s(t))]^{-1/2} \rangle , \quad (13)$$

where $e = L/2\pi a$.

The parameter describing the force-free field α will be replaced by a quantity normalized with respect to q^*,

$$\Gamma = \alpha R_o q^* , \quad (14)$$

so that the parameters that determine the equilibrium state of the plasma are : β/ε, q^* and Γ.

The effect of the ordering on the differential equation (3) is readily seen by writing it out in components; to leading order $\hat{B}_\phi$ is constant and $\hat{B}_r$, $\hat{B}_z$ are of $O(\varepsilon)$. Introducing a flux function for the poloidal field,

$$\underline{\hat{B}}_p = -\hat{e}_\phi \times \underline{\nabla}\bar{\psi} = -\hat{e}_z \frac{\partial \bar{\psi}}{\partial R} + \hat{e}_R \frac{\partial \bar{\psi}}{\partial z} , \quad (15)$$

the ϕ-component of (3) in the dimensionless coordinate system yields,

$$\nabla^2 \psi = \frac{\partial^2 \psi}{\partial x^2} + \frac{\partial^2 \psi}{\partial y^2} = -\Gamma , \quad (16)$$

where $\psi = \dfrac{q^* \bar{\psi}}{a \varepsilon B_o}$.

The boundary conditions to be imposed are (Eqs. (10) and (15)):

$$\underline{n} \cdot \underline{\nabla}\psi = -\hat{b}_p(t)$$

$$\psi = 0 , \quad (17)$$

on S.

The solution to the equilibrium problem has been reduced to a Poisson equation but with Cauchy boundary conditions, thus resulting into an ill-posed problem (see e.g. Ref. 4). Physically this means that the solution becomes sensitive to the boundary data, the more so the further one is removed from the surface on which these data are prescribed.

In the next section it is shown that for a large class of cross-sections this problem has an analytical solution. However, as we shall see this does not mean that the ill-posed character of the solution has been removed.

3. SOLUTION TO THE ILL-POSED PROBLEM

In the preceeding section is was shown that the equation describing the field in the force-free current region is a simple Poisson equation with Cauchy boundary conditions on S. In this section we show that an analytic continuation of the boundary data enables us to obtain the solution in an analytic form. This method was employed in Ref. 3 to arrive at the solution in a vacuum region.

First we reformulate the problem so that the equation reduces to the Laplace equation. This is accomplished by the introduction of another flux function:

$$\psi^H = \psi - \psi^P , \qquad \psi^P = -\frac{\Gamma}{4}(x^2 + y^2) . \tag{18}$$

so that in terms of this function the problem reads:

$$\nabla^2 \psi^H = 0$$

$$\text{on } S \begin{cases} \underline{n} \cdot \underline{\nabla}\psi^H = \underline{n} \cdot \underline{\nabla}\psi - \underline{n} \cdot \underline{\nabla}\psi^P \\ \psi^H = -\psi^P \end{cases} . \tag{19}$$

To ψ^H there correspondents a magnetic field given by

$$B_x^H = + \frac{\partial \psi^H}{\partial y} , \qquad B_y^H = - \frac{\partial \psi^H}{\partial x} . \tag{20}$$

Because ψ^H is a solution to Laplace's equation it is harmonic and there exists a conjugate potential χ^H related to it by the Riemann conditions:

$$\frac{\partial \chi^H}{\partial x} = \frac{\partial \psi^H}{\partial y} \quad \text{and} \quad \frac{\partial \chi^H}{\partial y} = - \frac{\partial \psi^H}{\partial x} . \tag{21}$$

As is well known from the theory of complex variables we can express B^H in terms of a complex potential.

$$\begin{aligned} \phi(z) &= \chi^H + i\psi^H , \\ \bar{B}_z^H &= B_x^H - iB_y^H = \frac{d\phi}{dz} . \end{aligned} \tag{22}$$

The notation $\bar{A}$ designates the complex conjugate of A.

The method of Kerner et al. [3] is based on the fact that when S is given in a parametric form the conformal mapping - which maps the region outside S in the z-plane onto a semi-infinite strip in the ω-plane - is known (see figures).

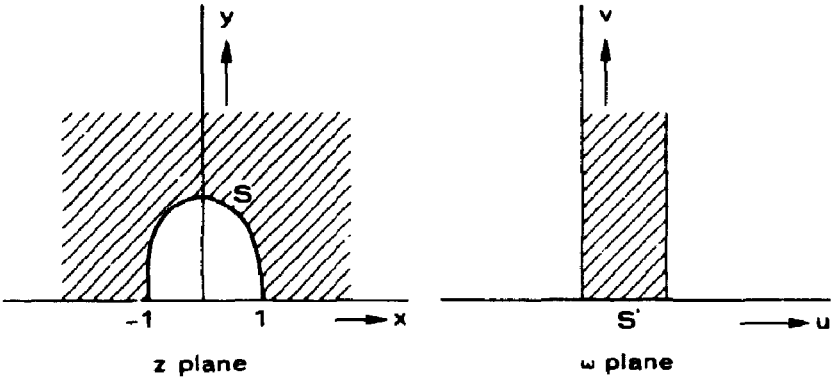

Let S be given by

$$x = f(t) \ , \qquad y = g(t) \ , \tag{23}$$

where t takes on the values between zero and 2π. The desired mapping is:

$$z = h(\omega) = f(\omega) + ig(\omega) \ , \tag{24}$$

where t is replaced by $\omega = u + iv$. By putting $v = 0$ we see that $h(\omega)$ maps S onto S'. Clearly f and g must be well-behaved otherwise $h(\omega)$ is not analytic and consequently the mapping not conformal. The theory of conformal transformations teaches that $\Phi(z(\omega))$ is also a solution to Laplace's equation and that we can define a field quantity $\bar{B}_\omega$ in the ω-plane that is related to $\bar{B}_z$ through:

$$\bar{B}_z = \frac{d\Phi}{dz} = \bar{B}_\omega \frac{1}{h'(\omega)} \ . \tag{25}$$

Another consequence of the mapping is that $u = u(x,y)$ and $v = v(x,y)$ correspond to an orthogonal coordinate system in the z-plane except at those points where $h'(\omega) = 0$, i.e., at the points where the mapping is not conformal, and that they satisfy the Cauchy-Riemann relations. It will be advantageous to replace $\bar{B}_z$ by a complex field quantity composed of the field components along the u,v-coordinates in the z-plane:

$$\bar{B}_{u,v} = B_u - iB_v = \frac{\underline{B} \cdot \underline{\nabla} u}{|\underline{\nabla} u|} - i\frac{\underline{B} \cdot \underline{\nabla} v}{|\underline{\nabla} v|} = \bar{B}_z \left[\frac{\partial u}{\partial x} - i\frac{\partial v}{\partial x}\right] g(u,v) \quad ,$$

where (26)

$$|\underline{\nabla} u| = |\underline{\nabla} v| = \sqrt{\left(\frac{\partial u}{\partial x}\right)^2 + \left(\frac{\partial u}{\partial y}\right)^2} = \sqrt{\left(\frac{\partial v}{\partial x}\right)^2 + \left(\frac{\partial v}{\partial y}\right)^2} = \frac{1}{\sqrt{h'(\omega)\bar{h}'(\bar{\omega})}} = \frac{1}{g(u,v)} .$$

The notation $\bar{h}(\omega)$ stands for $\bar{h}(\omega) = f(\omega) - ig(\omega)$ and is different from the complex conjugate of $h(\omega)$: $\overline{h(\omega)} = \bar{h}(\bar{\omega})$.
From (24) it is seen that (26) reduces to

$$\bar{B}_{u,v} = \sqrt{\frac{h'(\omega)}{\bar{h}'(\bar{\omega})}}\, \bar{B}_z \quad . \tag{27}$$

Combining (25) and (27) we obtain the following relationship between $\bar{B}_{u,v}$ and $\bar{B}_\omega$:

$$\bar{B}_\omega = \sqrt{h'(\omega)\,\bar{h}'(\bar{\omega})}\, \bar{B}_{u,v} \quad . \tag{28}$$

Since $\bar{B}_{u,v}$ is known on S ($v = 0$) and $\bar{B}_\omega$ is an analytic function of ω it is clear that the solution of $\bar{B}_\omega$ in the ω-plane can simply be obtained by a straightforward analytical continuation of the boundary data. On S' we have

$$\bar{B}_\omega(u, v=0) = \sqrt{h'(u, v=0)\,\bar{h}'(u, v=0)}\, \bar{B}_{u,v}(u, v=0) \quad , \tag{29}$$

so that by an analytical continuation we obtain

$$\bar{B}_\omega(\omega) = \sqrt{h'(\omega, v=0)\,\bar{h}'(\omega, v=0)}\, \bar{B}_{u,v}(\omega, v=0) \quad . \tag{30}$$

Applying (28) in the reverse direction we arrive at the solution of $\bar{B}_{u,v}$ in the original plane:

$$\bar{B}_{u,v} = \frac{\sqrt{h'(\omega, v=0)\,\bar{h}'(\omega, v=0)}}{\sqrt{h'(\omega)\,\bar{h}'(\bar{\omega})}}\, \bar{B}_{u,v}(\omega, v=0)$$

$$= \sqrt{\frac{\bar{h}'(\omega)}{\bar{h}'(\bar{\omega})}}\, \bar{B}_{u,v}(\omega, v=0)$$

or taking the complex conjugate:

$$B_u + iB_v = \sqrt{\frac{\bar{h}'(\bar{\omega})}{h'(\omega)}} \left[B_u(\bar{\omega}, v=0) + i B_v(\bar{\omega}, v=0) \right] . \tag{31}$$

Thus by a conformal transformation and an analytic continuation of the boundary data in the ω-plane we have obtained an analytic expression for the field outside a curve S in terms of the field on S.

The problem at hand, to determine the field outside S in the presence of force-free currents, has been reduced to a form to which the above method can be directly applied (19). In terms of the complex field quantity the homogeneous part of the solution on S is:

$$B_u^H(u) + iB_v^H(u) = \hat{b}_p(u) - \hat{e}_v \cdot \underline{\nabla}\psi^P \Big|_{v=0} + i\hat{e}_u \cdot \underline{\nabla}\psi^P \Big|_{v=0} . \tag{32}$$

Substituting ψ^P and making use of the Cauchy-Riemann relations we see that the contribution of the particular solution can be put in the form:

$$-\hat{e}_v \cdot \underline{\nabla}\psi^P + i\hat{e}_u \cdot \underline{\nabla}\psi^P = -i\frac{\Gamma}{2}\sqrt{\frac{\bar{h}'(\bar{\omega})}{h'(\omega)}}\, h(\omega) . \tag{33}$$

The homogeneous field on S is thus:

$$B_u^H(u) + iB_v^H(u) = \hat{b}_p(u) - i\frac{\Gamma}{2}\sqrt{\frac{\bar{h}'(u)}{h'(u)}}\, h(u) . \tag{34}$$

To arrive at the total field in the physical plane outside S (V^{ff}) we substitute (34) into (31), replacing u by $\bar{\omega}$, and add to it the complex field arising from the particular solution, i.e., (33) with a minus sign. The resulting expression is:

$$B_u + iB_v = \sqrt{\frac{h'(\bar{\omega})}{h'(\omega)}}\, \hat{b}_p(\bar{\omega}) - i\frac{\Gamma}{2}\sqrt{\frac{\bar{h}'(\bar{\omega})}{h'(\omega)}} [h(\bar{\omega}) - h(\omega)] . \tag{35}$$

Based on the form of this solution several observations can be made:

a. it is independent of the equilibrium problem inside S, it depends only on the field along S and on Γ;

b. the force-free currents lead to a term proportional to Γ that has the required property of being zero on S;

c. the first term - the vacuum contribution - can give rise to two

classes of stagnation points (zeros in B) that can be branch points. The first class is formed by the zeros due to the shape only: $h'(\bar{\omega})$ being zero or $h'(\omega)$ being ∞. The other class, the zeros originating from $\hat{b}_p(\bar{\omega})$ depend on the shape and the distribution of $\hat{b}_p(\bar{\omega})$ along S, i.e., in our model on k. Whether the stagnation points are simple zeros or branch points obviously depends on whether the functions are single- or multi-valued. An odd zero in $h'(\bar{\omega})$ will lead to a singularity (branch point), while an even zero will lead to a simple zero in the field. Another possibility of creating a simple zero is to have an odd zero due to $h'(\bar{\omega})$ coincide with an odd zero from $\hat{b}_p(\bar{\omega})$. This might seem an unusual coincidence but in Appendix A it is shown to be more normal than would appear on the basis of this expression. The branchcuts starting at the singular points are not just mathematical entities to make the solution single-valued but are physical in the sense that currents run along them, i.e., the branchcut is a current surface. The solution might have other singularities, namely where $h'(\omega)$ is zero. In the cases that we shall consider such singularities do not play a role.

Our object was to evaluate the ψ-surfaces in V^{ff}. In the case of a vacuum the simplest way to arrive at such an expression was to make use of (25) and (28), i.e., $\bar{B}_\omega$ is an analytic function of ω. Since the addition of force-free currents invalidates this we must make use of B_u and B_v:

$$B_u = \hat{e}_v \cdot \underline{\nabla}\psi = \frac{1}{\sqrt{h'(\omega)\bar{h}'(\bar{\omega})}} \frac{\partial\psi}{\partial v}$$

$$B_v = -\hat{e}_u \cdot \underline{\nabla}\psi = -\frac{1}{\sqrt{h'(\omega)\bar{h}'(\bar{\omega})}} \frac{\partial\psi}{\partial u} \,. \tag{36}$$

The value of ψ at u,v can thus be obtained by a simple integration along u = constant:

$$\psi(u,v) = \int_0^v dv \left[\mathrm{Re}\left\{\sqrt{h'(\bar{\omega})\bar{h}'(\bar{\omega})}\,\hat{b}_p(\bar{\omega})\right\} + \frac{\Gamma}{2}\,\mathrm{Im}\left\{\bar{h}'(\bar{\omega})\left[h(\bar{\omega}) - h(\omega)\right]\right\}\right] \tag{37}$$

Near the stagnation points such a single integration is often not possible. There one must be aware on which side of the branchcut ψ is sought and an extra integration along v = constant may be needed.

4. FLUX SURFACES OUTSIDE A CIRCULAR, ELLIPTICAL AND A D-SHAPED CROSS-SECTION

For a number of different plasma cross-sections and for various conditions the solution for the fields in the force-free field region, obtained in the previous section, is here employed to evaluate the flux surfaces.

From the pressure balance relation across S we have found (10) that the poloidal field on S has the form:

$$\hat{b}_p(t) = -\underline{n} \cdot \underline{\nabla}\psi = C_p\sqrt{1 - k^2/2\left(1 - x_s(t)\right)} \tag{38}$$

where $C_p = 1/\langle\sqrt{1 - k^2/2\left(1 - x_s(t)\right)}\rangle$

The shapes of S that are of primary interest are those that were considered in the stability analysis [1,6]. These shapes are described by the parametric form:

$$\begin{aligned} x &= \cos(t + c\sin t + d\sin 2t) \ , \\ y &= b\sin t \ , \end{aligned} \tag{39}$$

where the parameter t is an angle-like variable with values between zero and 2π. Since all shapes are symmetric with respect to the x-axis the range of t can be restricted to $0 - \pi$. The coefficients b, c and d have the following physical meaning: b corresponds to the height or elongation of the cross-section, c to the D-shape character and d to the race-track shape of S. By means of Eqs. (24), (35), (38) and (39) we are now in a position to evaluate the flux at any desired point outside the plasma surface S. Since every shape has its own complications we shall discuss the results by starting with the most simple shape, the circle, and then consider the ellipse and the D-shape.

THE CIRCLE

The parametric representation for the circle leads to the mapping

$$z = h(\omega) = \cos\omega + i\sin\omega = e^{i\omega} = e^{-v}(\cos u + i\sin u) \ , \tag{40}$$

so that in terms of the u,v coordinates a point in the z-plane is given by:

$$x = e^{-v}\cos u \ ,$$

$$y = e^{-v}\sin u \ .$$

From (35) and (38) the components of the poloidal field along the u,v coordinates given by (40) are seen to be:

$$B_u + iB_v = C_p\sqrt{\frac{h'(\bar{\omega})}{h'(\omega)}}\sqrt{1-\frac{k^2}{2}(1-\cos\bar{\omega})} - i\frac{\Gamma}{2}\sqrt{\frac{\bar{h}'(\bar{\omega})}{h'(\omega)}}[h(\bar{\omega}) - h(\omega)]. \quad (41)$$

Note that the unit vector along the v-coordinate is in the negative $\underline{n}$-direction (32), i.e., points outside S correspond to negative values of v.

The mapping is so simple that it is immediately clear that the only stagnation point arising from it is at infinity and does not affect the fields near S. The only stagnation point that plays a role arises from $\hat{b}_p(\bar{\omega})$ being zero:

$$\begin{aligned}\hat{b}_p(\bar{\omega}) &= C_p\sqrt{1-\frac{k^2}{2}(1-\cos\bar{\omega})} = 0 \ , \\ &= C_p\sqrt[4]{A^2+B^2}\ \exp\left[\frac{i}{2}\arctan(B/A)\right] \ ,\end{aligned} \quad (42)$$

where $A = 1 - \frac{k^2}{2}(1-\cos u\cosh v)$, $B = \frac{k^2}{2}\sin u\sinh v.$, and is located at:

$$u = \pi \ , \quad \cosh v = 2/k^2 - 1 \ , \quad (43)$$

where v should be taken negative. The interpretation of this stagnation point is straightforward. Without force-free currents, $\Gamma = 0$, there should be a stagnation point on the inside of the cross-section due to the toroidal character of the problem, i.e., $y_p = 0$ and negative x_p. When u and v given by (43) are converted into x and y by means of the mapping this point is found to lie at:

$$y_p = 0 \ , \quad x_p = 1 - \frac{2}{k^2} - \frac{2}{k^2}\sqrt{1-k^2} \ . \quad (44)$$

The behaviour of the stagnation point with k is as it should be: for low values of k, $\beta = O(\varepsilon^2)$, the point lies at $x = -\infty$, while for $k = 1$ it moves onto the plasma surface $x = -1$ so that the equilibrium limit is reached.

The stagnation point is not simply a zero point in the poloidal field, but a branchpoint as is seen from (41). How do the flux surfaces behave in the neighbourhood of this point? Near x_p the vacuum fields are given by:

$$B_u + iB_v = C^* \sqrt[4]{A^2 + B^2} \exp\left[\frac{i}{2} \arctan(B/A)\right], \qquad (45)$$

where the value of $\sqrt{\frac{h'(\bar{\omega})}{h'(\omega)}}$ at this point has been absorbed in C^*. From the expressions for A and B it is seen that B is negative for positive y and positive for negative y, while A is positive for $x > x_p$ and negative for $x < x_p$. The above expression can thus be simplified to:

$$B_u + iB_v = C^* \sqrt{\frac{k^2}{4}\left(1 - \frac{1}{x_o^2}\right)} \sqrt{s}\, e^{-i\theta/2}, \quad s \ll 1, \qquad (46)$$

where s and θ are indicated in figure a.

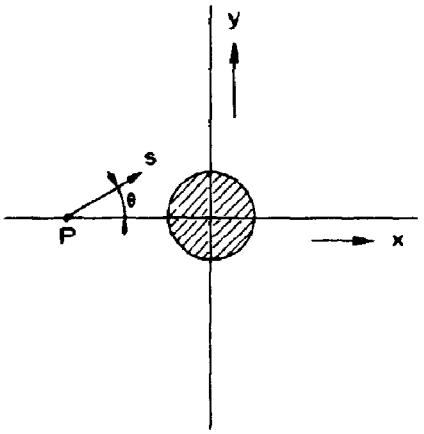

Figure a.

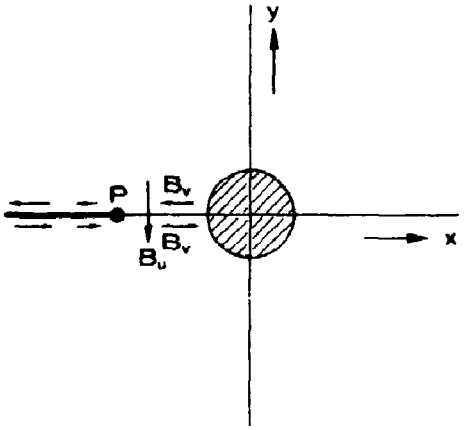

Figure b.

Keeping in mind that u is something like an angle around the origin and v is negative outside s, this equation shows that the distribution of the fields along the x-axis near x_p is as indicated in figure b. For x larger than x_p the field component parallel to the x-axis goes tc zero on this axis, as it should because the flux surfaces should be symmetric with respect to the x-axis. Beyond the stagnation point, however, this is not true anymore; there the field component B_v is not zero and changes sign when going from $y = +\varepsilon$ to $y = -\varepsilon$. Consequently, there must be a current layer from $x = x_p$ to $x = -\infty$. The other field component B_u is finite and proportional to $\sqrt{s}$ when $\theta = 0$ but for $x < x_p$ this component is zero. Thus, flux lines do not cross the x-axis when $x < x_p$. Since x_p is a zero point of the field, the current in the layer along

the x-axis must have the same dependence on s as B_v, i.e., in the neighbourhood of x_p it is proportional to $\sqrt{s}$. Another point that should be observed is that although B_u goes to zero when $x \to x_p$ ($x > x_p$) the derivative of the field with respect to x goes to infinity. The current in the layer has the same direction as the surface current in the plasma, it creates the vertical field needed to keep the plasma as a whole in equilibrium. Figure 1a shows the flux surfaces for a plasma with k = .9.

The replacement of the vacuum by force-free currents does not give rise to extra singularities. The contribution from these currents to the field is something like an extra poloidal field:

$$B_u^\Gamma + i B_v^\Gamma = -i \frac{\Gamma}{2} \frac{\overline{h'(\omega)}}{|h'(\omega)|} [h(\bar{\omega}) - h(\omega)] = -\Gamma \sinh v , \qquad (47)$$

namely everywhere a positive contribution to B_u. Consequently, is does affect the stagnation point: the field at x_p is not zero anymore but it does not move the sigular point to larger negative values of x as it would have had the zero point be a simple zero. Now the field on the -x-axis has everywhere a vertical component so that the stagnation point has disappeared and the field lines cross the x-axis. Together with the jump in the horizontal field component due to the current layer this results in a field structure along the x-axis as shown in Fig. 1b.

The influence of β and Γ on the field structure is now clear. With increasing β the stagnation point moves from $x = -\infty$ towards $x = -1$, and addition of force-free currents removes the stagnation point but does not remove the current layer along the branchcut of the corresponding vacuum case.

THE ELLIPSE

The ellipse in parametric form is

$$x = \cos t , \quad y = b \sin t , \qquad (48a)$$

so that the corresponding mapping and poloidal fields are

$$z = h(\omega) = \cos\omega + i b \sin\omega , \qquad (48b)$$

$$B_u + i B_v = C_p \sqrt{\frac{h'(\bar{\omega})}{h'(\omega)}} \sqrt{1 - \frac{k^2}{2}(1 - \cos\bar{\omega})}$$

$$- i \frac{\Gamma}{2} \sqrt{\frac{\overline{h'(\omega)}}{h'(\omega}} \left[h(\bar{\omega}) - h(\omega) \right] . \qquad (48c)$$

The difference in the fields in relation to the ones for the circle lies only in the mapping and thus in a different u,v-coordinate system in the z-plane.

Like in the case of the circle we first consider the vacuum solution ($\Gamma = 0$). The location of stagnation points due to the mapping is given by

$$h'(\bar{\omega}) = -\sin u(\cosh v + b \sinh v) - i \cos u(-\sinh v - b \cosh v) = 0$$

which results in the following possibilities for u and v:

$$\begin{aligned} &\text{a)} \quad u = 0 \text{ or } \pi , \qquad \sinh v + b \cosh v = 0 , \\ &\text{b)} \quad u = \frac{\pi}{2} \text{ or } \frac{3\pi}{2} , \qquad \cosh v + b \sinh v = 0 . \end{aligned} \tag{49}$$

The first one must be disregarded because the condition on v cannot be satisfied. The second class leads to two zero points on the y-axis, symmetric with respect to the axis, above and below S. In terms of y these points are located at:

$$y_q = \pm\left[b \cosh v - \sinh v\right] = \pm \frac{b^2 + 1}{\sqrt{b^2 - 1}} \quad ; \tag{50}$$

outside S v is negative. These two points move in along the y-axis from $\pm\infty$ toward $y = \pm b$ with increasing ellipticity. With an elongation $b = 2$ these points are located at $y_q = \pm 5/\sqrt{3} = \pm 2.89$.

The square root dependence of the field on $h'(\bar{\omega})$ means that the stagnation points are also branchpoints. The corresponding branchcuts are entirely determined by (48c). The dependence on $h'(\bar{\omega})$ implies that the difference $B_u + i B_v$ on the two sides of the branchcut is just a change in sig.. ($\Gamma = 0$). As across a current layer only the parallel field component can change sign this means that there is no field component normal to the branchcut and that it is a flux surface. To understand the behaviour of the branchcut with β we expand (48c) around the stagnation point. In terms of s and θ that are related to the u,v-coordinates by:

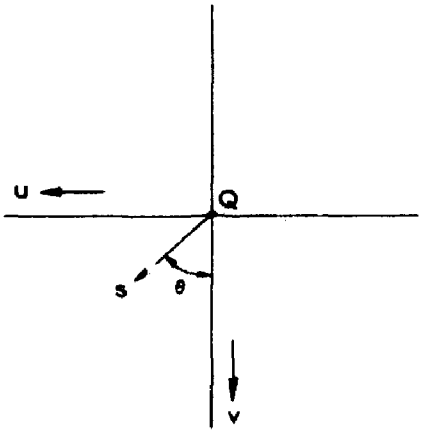

$$u = \pi/2 + s \sin\theta , \quad v = v_q + s \cos\theta ,$$

the vacuum field in the neighbourhood of Q is

$$B_u + iB_v = C_p \left[\frac{\sinh v_q + b\cosh v_q}{\cosh v_q - b\sinh v_q}\right]^{1/2} \sqrt{s}\, e^{i\theta/2} \sqrt{(1 - \frac{k^2}{2} + i\frac{k^2}{2}\sinh v_q)}\,, \tag{52a}$$

$$\equiv C_t \sqrt{s}\; e^{i(\theta-\Delta)/2}\,,$$

where the angle Δ is related to the value of k,

$$\Delta = -\arctan\left[\frac{k^2/2 \sinh v_q}{1 - k^2/2}\right]\,, \tag{52b}$$

and all other factors are absorbed in C_t. The condition that B should be parallel to the branchcut is:

$$B_u \cos\theta - B_v \sin\theta = 0\,, \tag{52c}$$

or by use of (52), $\cos(3\theta/2 - \Delta/2) = 0$.
This condition is satisfied by four angles,

$$\theta_1 = \pi/3 + \Delta/3,\ \theta_2 = -\pi/3 + \Delta/3,\ \theta_3 = \pi + \Delta/3,\ \theta_4 = -\pi + \Delta/3\,. \tag{53}$$

The reason for finding so many angles is that (53) only represents the condition that at an angle θ, B should be directed toward or from Q. For the branchcut we have the additional requirement that on both sides this direction should be opposite.

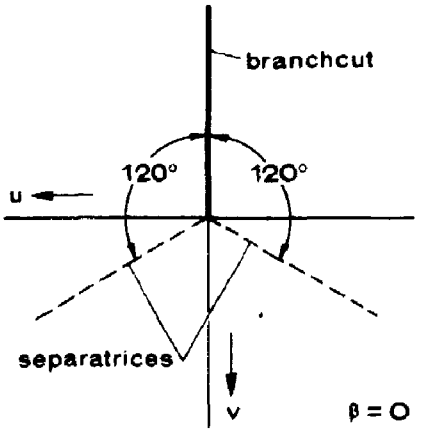

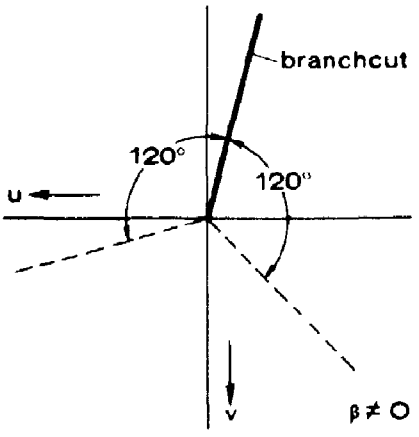

Clearly, θ_3 and θ_4 correspond to the two sides of the branchcut and the other angles refer to the separatrices that originate from this stagnation point. Thus the two separatrices make an angle of 120^o with each other no matter the value of k or the elongation [5]. At low-β, ($k \approx 0$), the toroidal effects are then negligible, the branchcut is vertical while with increasing values of k it undergoes a right-handed rotation (Figs. 2a,b).

The stagnation point from the analytical continuation of the poloidal field lies obviously at the same position in terms of u and v as in the case of the circle:

$$u = \pi \,, \quad \text{and} \quad \cosh v = 2/k^2 - 1 \,. \tag{54}$$

However, because of the mapping, this is at a different point in the z-plane. It is now located at:

$$y_p = 0 \,, \quad x_p = 1 - \frac{2}{k^2} - \frac{2b}{k^2}\sqrt{1 - k^2} \,, \tag{55}$$

which agrees with (44) for b = 1. The position of this point is a function of the elongation, the larger b the further away it is from the surface. Like for the circle this stagnation point is a branchpoint and the beginning of a current layer along the -x-axis, and it moves towards x = -1 with increasing k. Also the behaviour of the flux surfaces is the same (Fig. 2b).

The effect of the force-free currents is similar to that in the case of the circle. The extra term does not give rise to extra singularities and in a global way it means that in every point an extra poloidal field is added to the vacuum field. The branchcuts stay where they were at $\Gamma = 0$ and remain current surfaces through which the flux surfaces now pass (Fig. 2c).

D-SHAPED CROSS-SECTIONS

The parameter representation of S given by (39) is very well suited to describe a D-shaped surface. With d = 0, b still describes the height of the cross-section while c is directly related to the shift of the top of the D in the - or + x-axis direction (Fig. 3). The mapping corresponding to this representation is:

$$z = h(\omega) = \cos(\omega + c \sin\omega) + i b \sin\omega \,. \tag{56}$$

In the previous cases the stagnation points have complicated the numerical analysis of the flux surfaces but the location was readily determined analytically. For the circle there was only one, the one that arose from the analytical continuation of $\hat{b}_p$, while the ellipse had three such points: two from the mapping and one from $\hat{b}_p(\bar{\omega})$. In the case of the D-shape the number of stagnation points originating from the mapping has increased so much that a full analysis of the flux surfaces is useless. However, many of these lie far from S and affect the flux surfaces in a region which is of no interest. Therefore, we restrict ourselves to those stagnation points that only affect the fields near S.

Table I contains a list of stagnation points that arise from zeros of the mapping function for various D-shapes. From this table, together with the results for the circle and the ellipse, emerges the picture that the position of the points nearest to S are closely related to the curvature of S. The larger the curvature in a region, the closer a stagnation point.

The number of stagnation points arising from the analytic continuation of $\hat{b}_p(\bar{\omega})$ increases also and their behaviour with beta becomes more complex. The position of these points must satisfy:

$$1 - \frac{k^2}{2}\left[1 - \cos(\bar{\omega} + c \sin \bar{\omega})\right] = 0 . \qquad (57)$$

Assuming that there will be a point on the -x-axis, we look for solutions to (57) at $u = \pi$, i.e., v should be a solution to:

$$\cosh(v - c \sinh v) = \frac{2}{k^2} - 1 . \qquad (58)$$

While with $c = 0$ this equation can have only one solution for v, when c is finite the curve always changes its character and has a minimum and a maximum. The number of zeros can then be one or three depending on the value of k (Fig. 4). This would seem a strange behaviour and upon close examination is found not to be true; there are always three roots. For small values of k there is indeed one zero on the axis but there are also two roots off the axis, one above and one below. With increasing k the latter move towards the surface S and towards the axis. At that value of k for which (58) has exactly two solutions these roots coalesce on the x-axis and move apart along this axis upon further increase of k.

The influence of the D-shape on the root (from $\hat{b}_p$) nearest to S is seen to be as follows. Equation (58) shows that a positive value of c - an inward leaning D - results in a larger negative value of v. As

the x-coordinate of this point is given by:

$$x_p = \text{Real}\left(h(\omega = \pi + iv)\right) = -\cosh(v - c\sinh v) + b\sinh v\,,$$
$$= 1 - \frac{2}{k^2} + b\sinh v\,, \tag{59}$$

we have the same expression as for the ellipse. However, the value of v that belongs to this point is larger (negative) than the one for the ellipse (58) and thus results in a point further removed from S. In a sense this stagnation point behaves like the ones related to $h'(\bar{\omega})$, it is further removed from the surface the smaller the curvature.

The behaviour of the flux surfaces near the stagnation points with and without force-free currents is similar to that in the case of the ellipse (Figs. 5a,b).

5. THE STABILITY OF THE SCREW-PINCH

The previous sections all dealt with the determination of the magnetic fields outside a high-beta tokamak plasma. In this section the original question will be addressed: which combination of equilibrium parameters (β, q^* and Γ) gives rise to q-profiles that correspond to those of a screw-pinch.

In terms of the dimensionless poloidal field $\tilde{b}_p$, the safety factor q on a flux surface is,

$$q/q^* = \frac{1}{2\pi} \int d\ell^* \frac{1}{\tilde{b}_p} , \tag{60}$$

where $d\ell^*$ is an infinitesimal length along the ψ = constant surface in the dimensionless coordinates of the cross-section. Since the ψ-surface depends only on k (through the boundary condition) and Γ, the q/q^* versus ψ-profile has a similar dependence. The stability results [1,6] were displayed in $(\beta/\epsilon, q^*)$ plots. In such a figur the line k = const (11) corresponds to a hyperbola $\beta/\epsilon\, q^{*2}$ = constant. The dependence of q/q^* on k and Γ thus implies that on each $\beta/\epsilon\, q^{*2}$ = const line q/q^* does not vary.

In the figures 6a,b and 7a,b the q/q^* dependence on the flux surface has been plotted for the ellipse and the D-shape, that were analyzed in the previous section, for various values of k and Γ; the dependence on the flux has been replaced by the intersection points of these surfaces with the +x-axis. What do these figures tell us? Essentially two things. First, $\frac{dq}{dr}$ decreases with increasing Γ and with increasing k. More important is the observation that almost uniform q-profiles do exist so that the condition for having a screw-pinch can well be put in the form:

$$\frac{d}{d\psi} \left(q/q^* \right)_{\text{on } S} = 0 . \tag{61}$$

This condition is much simpler to implement than to evaluate q through the solution of the ill-posed problem as was carried out in the previous section. In fact, by employing the theory of section 3, we shall see that this condition can directly be transformed in a relationship between $\epsilon\beta_p$ (or k) and Γ.

In terms of the (u,v) coordinate system (in the z-plane) introduced in section 3 (60), on S, reads:

$$q/q^* = \frac{1}{2\pi} \int_S du \; \frac{q^2}{\frac{\partial \psi}{\partial v}} = \frac{1}{2\pi} \int_{v=0} du \; \frac{q}{\tilde{b}_p} , \tag{62}$$

where g(u,v) is given by (26). Because S is a magnetic surface coinciding with a coordinate surface (v = 0) differentiation with respect to ψ yields:

$$\frac{d}{d\psi}\left(q/q^*\right)_S = \frac{1}{2\pi}\int_S du\left[\frac{1}{\left(\frac{\partial\psi}{\partial v}\right)^2}\frac{\partial g^2}{\partial v} - \frac{g^2}{\left(\frac{\partial\psi}{\partial v}\right)^3}\frac{\partial^2\psi}{\partial v^2}\right] . \tag{63}$$

The second derivative of ψ with respect to v, on S, can be obtained from (16):

$$\frac{\partial^2\psi}{\partial v^2} = -\Gamma g^2 , \tag{64}$$

The equilibrium parameters, leading to a uniform q-profile, must thus satisfy

$$\frac{d}{d\psi}\left(q/q^*\right) = \frac{1}{2\pi}\int_o^{2\pi} du\left[\frac{1}{g^2\hat{b}_p^2}\frac{\partial g^2}{\partial v} + \Gamma\frac{g}{\hat{b}_p^3}\right] = 0 , \tag{65}$$

where $g^2 = \overline{h'(\omega)}\,h'(\omega)$. Clearly this results in a relation between $\varepsilon\beta_p$ (or k) and Γ, because $\hat{b}_p$ depends only on k. Figure 8 shows the results of a calculation for an ellipse with an elongation of 1.5. The points on this curve correspond to equilibrium parameters of a screw-pinch while for points above $\frac{dq}{d\psi}\Big)_S$ is negative and below it the derivative is positive.

Let us now impose the above condition on the equilibrium parameters for a high-beta tokamak and so arrive at the stability results for a screw-pinch. Fig. 9a depicts the marginal stability curves for an ellipse (b/a = 1.5) for various values of force-free currents. Since $\varepsilon\beta_p$ (= $\beta/\varepsilon q^{*2}$) is constant along the curve $(\beta/\varepsilon)q^{*2}$ = const, the radial q/q^* profile and therefore $\frac{dq}{d\psi}$ on S do not vary either. A point of Fig. 8 corresponds to a curve $(\beta/\varepsilon)q^{*2}$ = const, in Fig. 9a, so that the intersection of this with the curve for marginal stability corresponds to the marginal stable point of the screw-pinch. For the ellipse these points are indicated in Fig. 9a by the squares 1 to 3. The curves a, b, d, f mark the boundary of the stable region for the values of the FFC: $e\Gamma$ = 0, 1, 2 and 3. The points 1 to 3 are the marginal stable points for the screw-pinch with the following values of the FFC: $e\Gamma \approx 0.1$, 1, 1.5 and ~2 ($e = L/2\pi a$, L is the circumference). Above these points $\frac{dq}{d\psi}$ on S is negative while below them, on the curves of marginal stability $\frac{dq}{d\psi}$ on S is positive.

In the same manner the stability of the "screw-pinch" mode can be determined for other cross-sections. Figures 9b and 9c show the results for two D-shapes (c = 0.3 and 0.5) with the same elongation as the ellipse and the results for the same shapes but with an elongation b/a = 2 are shown in Figs. 10a, b and c. In analyzing these figures we must keep in mind that the model only approximates the experiment so that the "screw-pinch" mode points should really be given error bars. The figure shows that a large part of the stability diagram for each of these cross-sections is not available for the screw-pinch. The gain in beta due to the addition of FFC for a given cross-section is only slight although it permits one to increase the plasma current. The FFC should not be taken too large otherwise the marginal stable points for the screw-pinch mode of operation start to move to lower betas. Elongating the cross-section leads to an increase in beta. For the ellipse, however, one should not go further than b/a $\approx$ 2. The rapidly increasing curvature at the top of the ellipse leads to a decrease in beta for larger elongations. The favourable effect of elongating the cross-section is best retained when the cross-section is given a D-shape together with the elongation. This is seen from Table II where the maximum values of β/ε, obtained from the Figs. 9 and 10, are listed. Shaping the cross-section can almost double the maximum value of β/ε with respect to the one for the circle.

In the experiment one might well obtain higher values of beta because the q-profile might not be exactly uniform and the values obtained by the method employed in this report are quite sensitive to the values of $\frac{dq}{d\psi}$ on S. Furthermore, the effect of the wall on the stability might be quite appreciable. In the stability results presented in [1,6] this effect has been neglected.

6. CONCLUSIONS

To determine the combination of equilibrium parameters of a high-beta tokamak that gives rise to a screw-pinch equilibrium it was necessary to obtain the fields outside a plasma whose cross-section is prescribed. The high-beta tokamak ordering reduces this to a two-dimensional elliptic problem with Cauchy boundary conditions: an ill-posed problem. For a large class of plasma cross-sections this problem can be solved. By an analytic continuation of the boundary data one obtains an analytic expression for the poloidal field. The fields outside the plasma - in the surface current model of a high-beta tokamak - with various cross-sections have been determined by means of this solution. From these results it was concluded that the screw-pinch mode of operation of a high-beta tokamak - a uniform q-profile - can well be determined from the condition on the derivative of q on the plasma surface: $\left.\frac{dq}{d\psi}\right)_S = 0$. This leads to a simple integral condition from which the combination of equilibrium parameters that correspond to a screw-pinch can readily be determined by numerical means. For a number of plasma cross-sections this has been carried out and leads to "screw-pinch" points on the marginal stability curves in the stability diagrams (Figs. 9, 10). These figures show that the stable region in parameter space for the screw-pinch is much smaller than that for the high-beta tokamak with FFC. The effect of adding FFC is reduced because although it enlarges the stability region its effect through the equilibrium leads to smaller $\varepsilon\beta_p$, thus to smaller β's unless the first effect dominates. The best results are obtained for elongated cross-sections with a D-shape. A plasma with a D-shape: b/a = 2, c = 0.3 reaches a maximum stable beta of $.63\varepsilon$.

The form of the analytic solution for the magnetic field in the region surrounding the plasma suggests that a classification of the stagnation points in two groups - one arising from the shape of the cross-section (S) alone and one based on the distribution of the poloidal field over S ($\hat{b}_p$) - is useful. The analysis in Appendix A serves to point out the special nature of the surface current model in this respect. It is shown that for the case of a cylindrical plasma with a uniform current these two groups interact: the stagnation points from S coincide with those arising from $\hat{b}_p$. Therefore, it may not be concluded that the stagnation points - as is the case for the surface current model - are usually branch points and thus accompanied by surface currents. Were that the case they would impose a serious restriction on the shape of the cross-section and the beta of a plasma confined and held in equilibrium by a conducting shell. The plasma surface S would then not be permitted to take on a shape so that a corresponding stagnation point would lie within the shell. A

similar requirement on the stagnation point from $\bar{b}_p$ would lead to a limit on the plasma beta. Not only would this be true for a plasma surrounded by a vacuum but also in the presence of FFC. In the case of simple stagnation points this reasoning does not apply because these points are not accompanied by a branchcut carrying surface currents. Furthermore, FFC can always move such points to a location outside the shell.

The ill-posed problem appeared only because the plasma cross-section was specified. It could have been prevented by considering the free-boundary problem. This problem has been investigated in [7]. How do these two approaches compare? This has been investigated in Appendix B by approximating the plasma shape obtained from the free-boundary analysis by an analytic form that could serve as an input for the ill-posed problem. The magnetic fields surrounding the plasma thus obtained, do not agree with the ones from the free-boundary analysis. The treatment in Appendix B shows that the ill-posed character of the solution to the problem of the prescribed plasma shape has to do with the fact that the solution is sensitive to the higher harmonic content of the boundary conditions. Consequently, the analytical solution is useful for such purposes as encountered in this paper but otherwise should be used with care, in particular in the region where stagnation points occur. Only in the neighbourhood of the plasma surface is the solution insensitive to the higher harmonics of the boundary data. Obviously, the same comment applies to all analytic solutions, e.g., by means of expansions in a small parameter, of similar "ill-posed" problems.

ACKNOWLEDGEMENTS

The author would like to acknowledge the many fruitful discussions with Dr. J.P. Goedbloed.

This work was performed as part of the research programme of the association agreement of Euratom and the "Stichting voor Fundamenteel Onderzoek der Materie" (FOM) with financial support from the "Nederlandse Organisatie voor Zuiver-Wetenschappelijk Onderzoek" (ZWO) and Euratom.

REFERENCES

1. D.A. D'Ippolito, J.P. Freidberg, J.P. Goedbloed, and J. Rem, Phys. Fluids 21 (1978) 1600.

2. C. Bobeldijk et al., Rijnhuizen Report 78-112, *Proposal for a Modification of Spica*, (1978).

3. W. Kerner, D. Pfirsch and H. Tasso, Nuclear Fusion 12 (1972) 433.

4. P.R. Garabedian, *Partial Differential Equations*, Wiley, New York,1964.

5. R. Gajewski, Phys. Fluids 15 (1972) 70.

6. D.A. D'Ippolito, J.P. Freidberg, J.P. Goedbloed, and J. Rem, Proc. Finite-Beta Theory Workshop, Varenna, Italy (1977) 75.

7. J.P. Goedbloed, Proc. 9th European Conf. on Contr. Fusion and Plasma Phys.,Oxford (1979) 171.

A P P E N D I X A

SKIN CURRENT MODEL VERSUS DIFFUSE PLASMA CURRENTS

The method of finding the field distribution outside a given cross-section - developed in Sec. 3 - has been applied to the surface current model only. Below, it shall be investigated to what extent the observed features of the fields can be attributed to this special model.

As we have pointed out the method for determining the fields outside S is independent of the plasma equilibrium inside S. Therefore it applies to a diffuse equilibrium as well. However, to be of any use, the field on S as well as the surface S itself must be in an analytical form and the high-beta ordering must be applicable. The first two requirements are unfortunately not easily satisfied. Not surprisingly because the equilibrium of a diffuse plasma is a problem in its own right.

A model that is sufficiently different from the skin current model and meets the requirements mentioned above is that of a cylindrical plasma with a uniform current, zero beta and arbitrary cross-section, embedded in a strong parallel magnetic field. The fields inside and outside S again are described by flux functions that must satisfy:

$$V^p \qquad \nabla^2\psi^p = \Gamma^p \tag{1a}$$

$$S \qquad -\underline{n}\cdot\underline{\nabla}\psi^p = -\underline{n}\cdot\underline{\nabla}\psi^{ff}\,; \qquad \psi^p = \psi^{ff} = \text{const} \tag{1b}$$

$$V^{ff} \qquad \nabla^2\psi^{ff} = \Gamma^{ff} \tag{1c}$$

Before concluding that we must consider a special shape - even this simple problem is not tractable by analytic means for a general S - let us proceed as far as possible.

To determine the flux surfaces in V^{ff} we do not necessarily need ψ in V^p but only $\hat{b}_p$ on S, i.e., $\underline{n}\cdot\underline{\nabla}\psi^p$ on S. From (1b) and S in the form $y = y_s(x_s)$ we derive

$$\hat{b}_p = -\sqrt{1 + \left(\frac{dy}{dx}\right)_S^2}\ \left(\frac{\partial\psi^p}{\partial y}\right)_x \tag{2}$$

In terms of the mapping introduced before this is:

$$\hat{b}_p = \frac{-\sqrt{h'(u)\bar{h}'(u)}}{\left(\frac{\partial x}{\partial u}\right)_{v=0}}\ \left(\frac{\partial\psi^p}{\partial y}\right)_x \tag{3}$$

Is this a useful expression or does it only hide a dependence of $\frac{\partial\psi}{\partial y}\Big|_x$ or $\frac{\partial x}{\partial u}\Big|_{v=o}$ on $h'(u)$? Is after all the following expression:

$$\hat{b}_p = -\underline{n}\cdot\underline{\nabla}\psi^p = \frac{1}{\sqrt{h'(u)\bar{h}'(u)}}\frac{\partial\psi^p}{\partial v}\Big|_{v=o} \tag{4}$$

not better? Substitution in (35) clearly leads to different conclusions about the presence and the nature of the stagnation points arising from the mapping. The last expression (4) even suggests that there is no stagnation point due to $h'(\bar{\omega})$. The surface current model has shown that such points do exist, and on that basis we can disregard (4). However, also the first expression for $\hat{b}_p$ suggests something different. On the basis of this we might conclude that the stagnation points due to $h'(\bar{\omega})$ are simple, i.e., not accompanied by branchcuts carrying currents. Although this is not true for the skin current model it is true for the cylinder with an elliptic cross-section and a uniform current distribution [5].

To proceed further we consider a shape related to the ellipse with a uniform current but one that is more general. The cross-section S given by

$$C_1x^2 + C_2y^2 + C_3(x^4 - 6x^2y^2 + y^4) = 1 \tag{5}$$

was used in [1] to describe a racetrack and permits an analytic solution of (1a):

$$\psi^p = \frac{\Gamma^p}{2(C_1 + C_2)}\left[C_1x^2 + C_2y^2 + C_3(x^4 - 6x^2y^2 + y^4) - 1\right] . \tag{6}$$

This solution is obtained by employing the requirement that a solution to (1a) must be of the form:

$$\psi^p = f(z) + \bar{f}(\bar{z}) + \frac{\Gamma^p}{4} z\bar{z} . \tag{7}$$

To obtain from this the solution of the fields in V^{ff} is straightforward. Through (3) we obtain $\hat{b}_p$ along S and the fields in V^{ff} are obtained by the same method as before: an analytic continuation of the boundary data. *In writing $\hat{b}_p$ in (3) we left the point open what u stood* for. In the case of the surface current model it was an angle-like parameter. Here, S is not in a parameter form. The simplest way to bring it in such a form is to write (5) in polar coordinates:

$$C_3 r^4 \cos 4\theta + r^2 (C_1 \cos^2\theta + C_2 \sin^2\theta) - 1 = 0 . \qquad (8)$$

The solution of r in terms of θ can be carried out so that $r = r(\theta)$ is known explicitly. A suitable mapping is thus:

$$x + iy = h(\omega) = r(\omega)\, e^{i\omega} . \qquad (9)$$

Making use of (6), (8) and (9) $\hat{b}_p$ from (3) can be shown to reduce to:

$$\hat{b}_p(\theta) = \sqrt{h'(\theta)\bar{h}'(\theta)}\ \frac{\Gamma^p}{(C_1 + C_2) r^2}\ (C_3 r^4 \cos 4\theta + 1) . \qquad (10)$$

Analytical continuation of this field yields the following expression for the vacuum field outside S (35):

$$B_u + i B_v = \frac{h'(\bar{\omega})}{h'(\omega)}\ \sqrt{h'(\omega)\bar{h}'(\bar{\omega})}\ \frac{\Gamma^p}{(C_1 + C_2) r^2(\bar{\omega})}\ [C_3 r^4(\bar{\omega}) \cos 4\bar{\omega} + 1] . \qquad (11)$$

Since the zeros of $h'(\bar{\omega})$ do not coincide with those of $r^2(\bar{\omega})$ this expression proves that these points correspond to simple stagnation points and not to branch points. In the case of the surface current model the zeros would be at the same points but would be branch points. The field on S for this model is namely a constant so that

$$(B_u + i B_v) \sim \sqrt{\frac{h'(\bar{\omega})}{h'(\omega)}} \qquad (12)$$

To complete this section we consider the ellipse with a uniform current. This is a special case of the one just treated that has the advantage of leading to a simple expression for the fields in V^{ff}. Instead of using (11) - which leads to complicated expressions - we use the mapping employed in Sec. 3:

$$\hat{b}_p = \sqrt{h'(u)\bar{h}'(u)}\ \frac{b\Gamma^p}{b^2 + 1} , \qquad (13)$$

so that the field in V^{ff} takes on the simple form

$$B_u + i B_v = \frac{h'(\bar{\omega})}{h'(\omega)}\ \sqrt{h'(\omega)\bar{h}'(\bar{\omega})}\ \frac{b\Gamma^p}{b^2 + 1} . \qquad (14)$$

This expression confirms the conclusions reached before. The stagnation

points from the mapping coincide with those for the surface current model but are now only simple zeros. By expanding around a stagnation point we find that the two separatrices intersect and cross each other perpendicular and like in the surface current model this angle is independent of the elongation.

A P P E N D I X B

FIXED-BOUNDARY VERSUS FREE-BOUNDARY ANALYSIS

The problem treated in this paper is ill-posed because the plasma cross-section is prescribed. In the toroidal screw-pinch "Spica" the equilibrium of the plasma is actually a free-boundary problem. A good conducting shell determines the shape of the outermost magnetic surface and the confined plasma - surrounded by force-free currents - takes on the shape needed for equilibrium. For the same plasma model as was considered here such a free-boundary analysis was carried out (7). A high-beta tokamak plasma surrounded by a vacuum region was confined by a circular conducting shell. The shape of the plasma and the position with respect to the shell were determined as function of beta. The following question now arises: how do the two equilibrium analyses compare? A comparison was made as follows. A certain plasma shape and beta were taken from the free-boundary analysis and used as input for the method developed in section 3 to evaluate the field outside (Fig. 11). The fact that we considered only shapes representable by (39) means that an accurate representation of S in this form is not really possible. The parameter combination:

$$b = 1.38 \quad c = .1268 \quad d = 0.04 \quad \text{and} \quad k = .955$$

is found to lead to an S close to the one given. When the stagnation points corresponding to this solution are plotted (P,Q) we see immediately that both points fall within the shell (Fig. 11). In terms of the dimensionless coordinates of S these points are located at:

$$\text{stagnation point shape: } x_Q = -1.2 \quad y_Q = \pm 2.25$$
$$\text{" " " " beta: } x_P = -2.47 \quad y_P = 0.0 .$$

Clearly the two methods do not give the same result. How must this be understood? Although the approximation to the surface looks good it is rather poor when the corresponding Fourier representations are considered. The difference lies in the higher order components. It is exactly this difference that plays a role in the ill-posed problem. The solution is sensitive to the higher harmonics. This can be shown very simply by first Fourier analysing S:

$$x = r(\theta)\cos\theta \cdot \quad y = r(\theta)\sin\theta$$
$$r(\theta) = \sum_{m=0}^{\infty} \sigma_m(\theta)\cos m\theta \qquad (1)$$

and then applying the method of section 3 with the mapping

$$h(\omega) = r(\omega)\, e^{i\omega} \qquad (2)$$

to obtain the fields outside S. Applied to the ellipse we observe: the original stagnation point is further away from the surface when only a few harmonics are taken and other spurious stagnation points appear. The latter are more numerous and closer to S when more harmonics are taken into account (Table III). Based on this observation we must conclude that our method of determining the fields outside a cross-section S on which the poloidal field is given cannot claim to yield "the" solution. The ill-posed character of the problem makes that the solution is sensitive to the higher harmonics of the surface, especially far away from S. All that can be said is that the analytic solution is close to the "correct" solution in the neighbourhood of the surface.

Table I

stagnation points arising from $h'(\bar{\omega}) = 0$ for various D-shapes			
elongation b/a	D-shape c	stagnation points	
1.5	0	x = 0	y = ±2.9
1.5	0.3	x = 3.31	y = 0.0
		x = -37.1	y = 0.0
		x = -.816	y = ±2.10
2.0	0	x = 0	y = ±2.887
2	0.1	x = 13.43	y = 0.0
		x = -.289	y = ±2.82
2	0.2	x = 7.27	y = 0.0
		x = -.494	y = ±2.69
		x = -7.25	y = ±24.11
2	0.3	x = 5.28	y = 0.0
		x = -.625	y = ±2.56
		x = -51.5	y = 0.0

Table II

maximum betas for the screw-pinch			
cross-section	elongation b/a	D-shape	$\beta/\%$
circle	1		0.38
ellipse	1.5		0.52
"	2		0.58
"	3		0.53
D-shape	1.5	c = 0.3	0.52
"	2	c = 0.3	0.63

Table III

Stagnation points for ellipse b/a = 1.5 with S given by a Fourier series		
$m \leq 5$	$x_Q = 0.0$	$y_Q = \pm 3.95$
	$x_{II} = \pm 2.66$	$y_{II} = 0.0$
$m \leq 10$	$x_Q = 0.0$	$y_Q = \pm 3.10$
	$x_{II} = \pm 2.19$	$y_{II} = 0.0$
	$x_{III} = \pm 2.29$	$y_{III} = \pm 1.07$

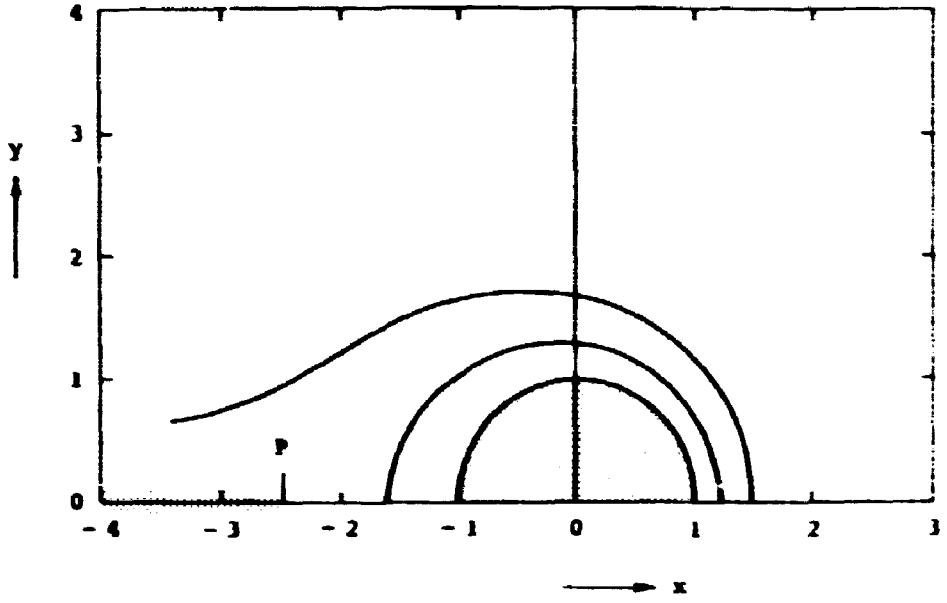

$\varepsilon\beta_p$ = .3639 (k = .9); no force-free currents

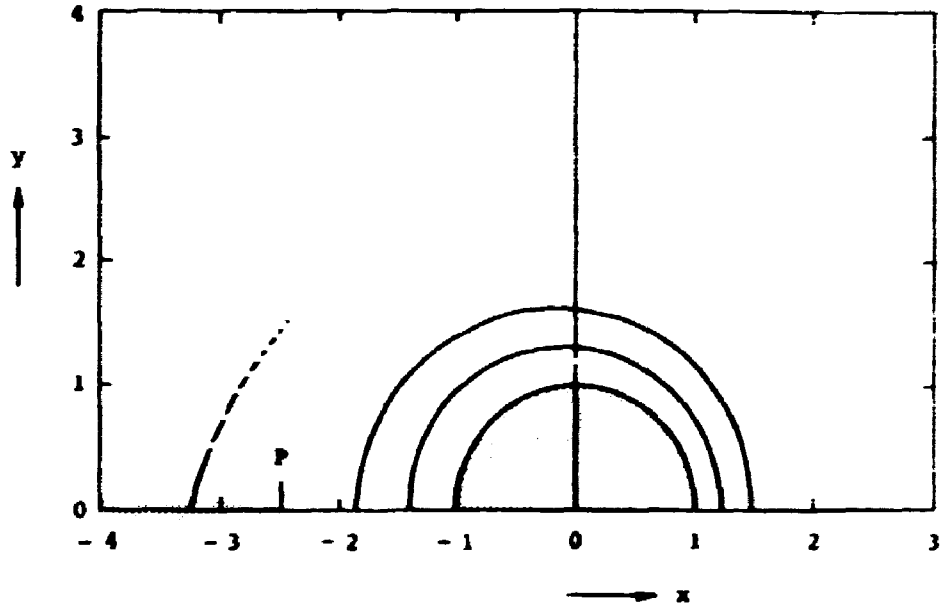

$\varepsilon\beta_p$ = .3639 (k = .9); Γ = 1.

Figs. 1: Flux surfaces around a high-beta tokamak plasma with a circular cross-section.

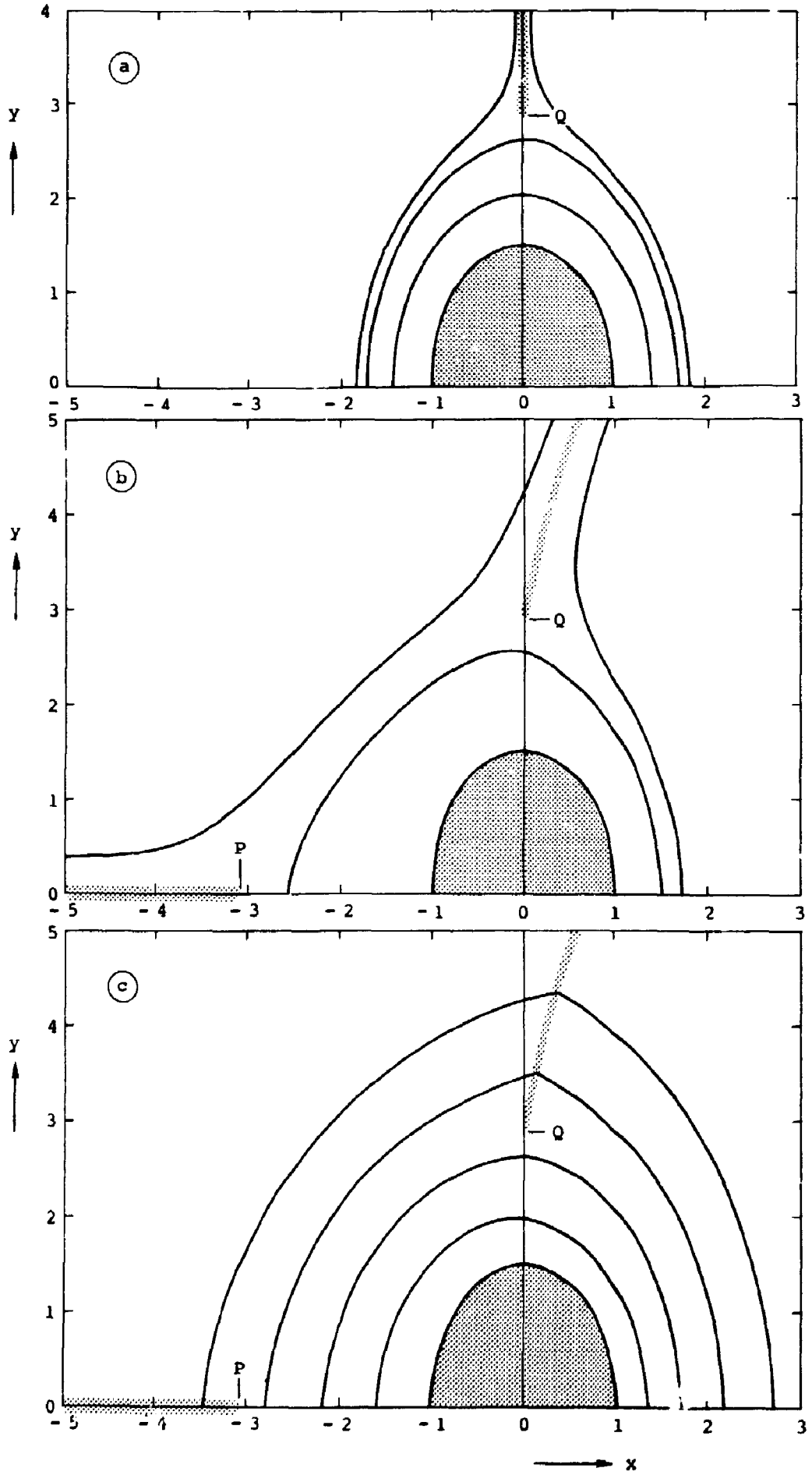

Figs. 2: Flux surfaces around a high-beta tokamak plasma with an elliptical cross-section (b/a = 1.5, e = L/2π = 1.262).

a) $\varepsilon\beta_p$ = 0.0 (k = 0); $e\Gamma$ = 0.0, b) $\varepsilon\beta_p$ = .366 (k = .9); $e\Gamma$ = 0.0,

c) $\varepsilon\beta_p$ = .366 (k = .9); $e\Gamma$ = 1.

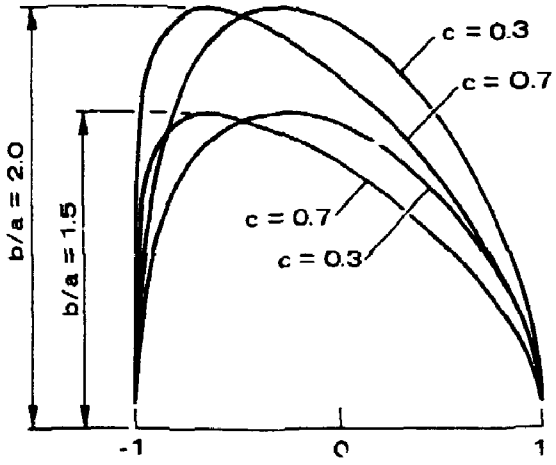

Fig. 3: D-shaped cross-sections given by the parameter representation (39) for two values of c and two elongations.

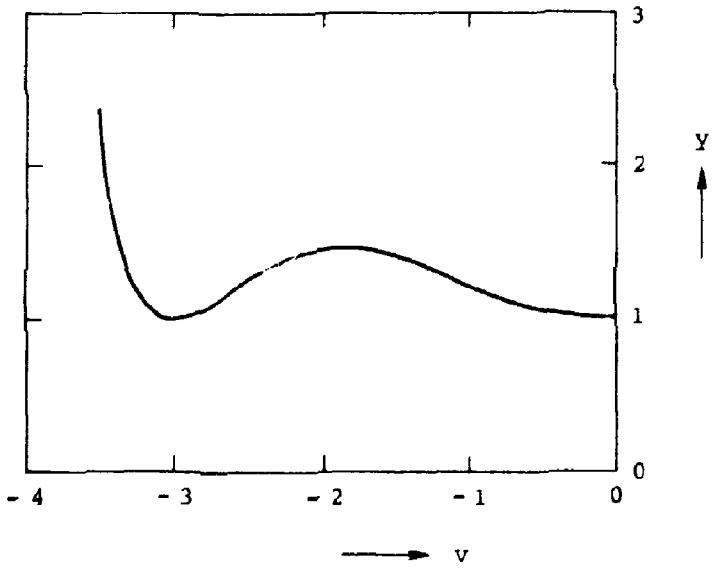

Fig. 4: Function $y = \cosh(v - c \sinh v)$, for $c = .3$.

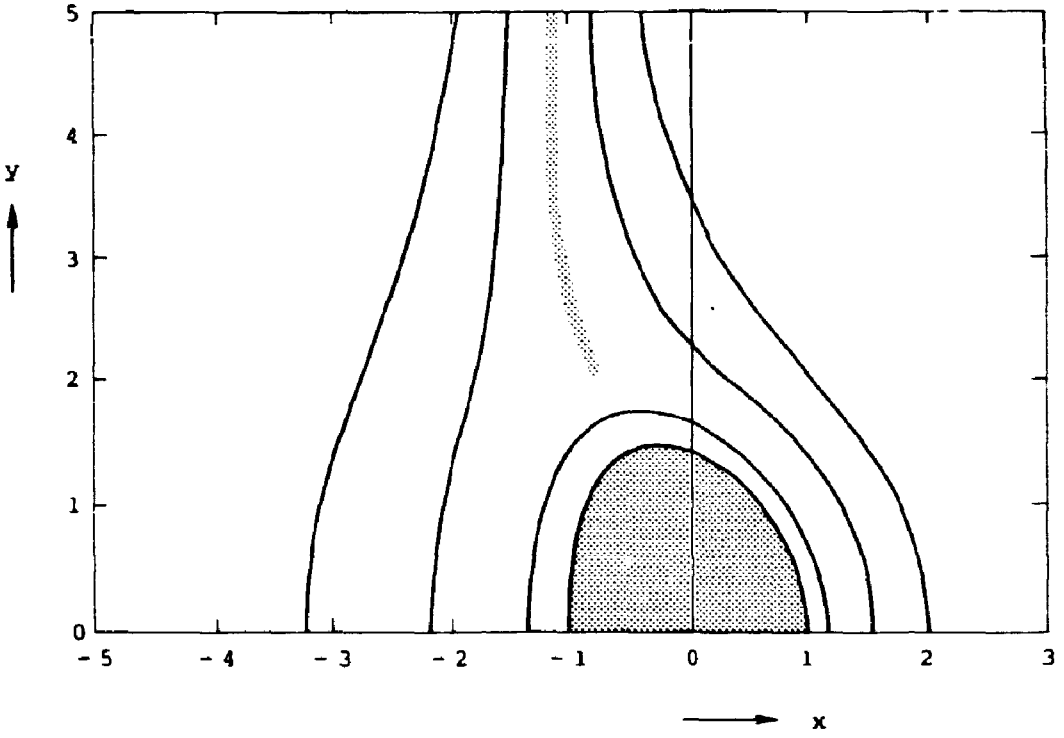

$\varepsilon\beta_p$ = .392 (k = .9); $e\Gamma$ = 0.

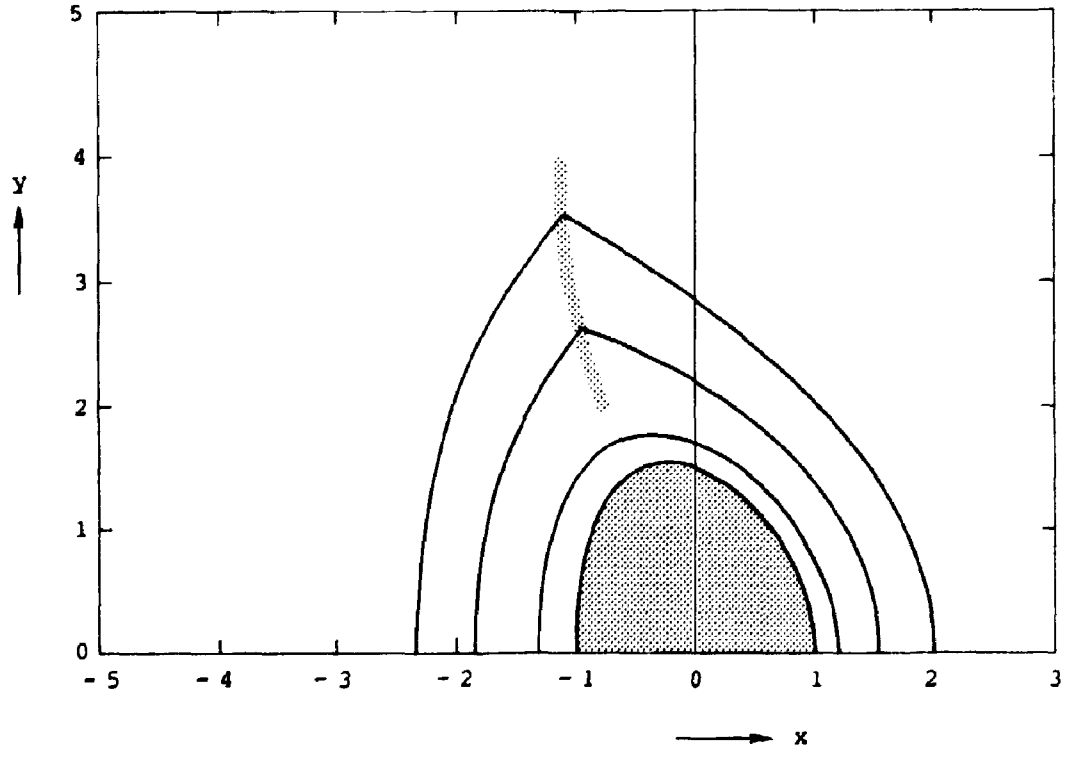

$\varepsilon\beta_p$ = .392 (k = .9); $e\Gamma$ = 1.0 .

Figs. 5: Flux surface around a high-beta tokamak plasma with a D-shaped cross-section (b/a ≈ 1.5, c = .3, e = L/2π = 1.267).

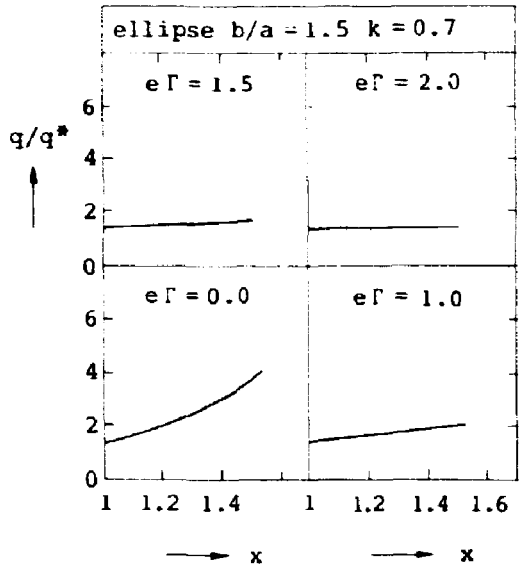

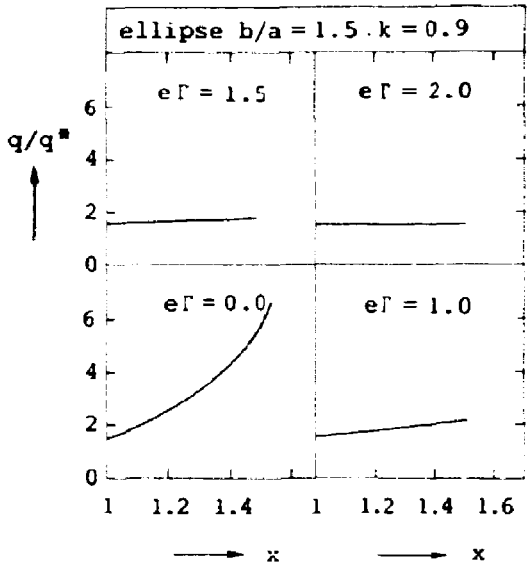

Figs. 6: q-profiles in the FFC region outside a high-beta tokamak plasma with an elliptical cross-section for various values of Γ (b/a = 1.5, e = L/2π = 1.262) and for two values of $\varepsilon\beta_p$: $\varepsilon\beta_p$ = .165 (k = 0.7) and $\varepsilon\beta_p$ = .366 (k = .9). The x-coordinate of a point corresponds to the intersection of a ψ-surface with the x-axis (see Fig. 1).

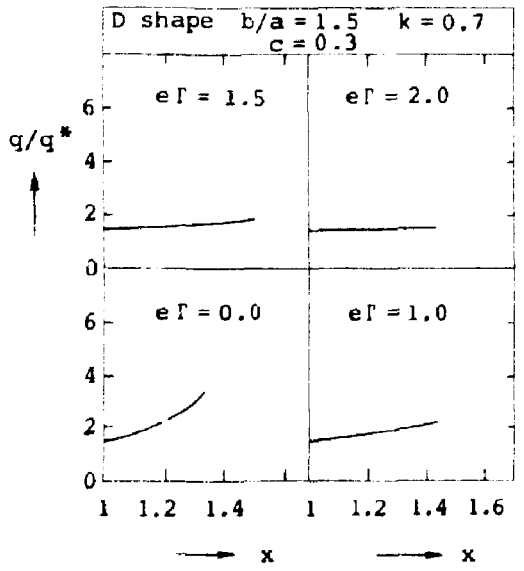

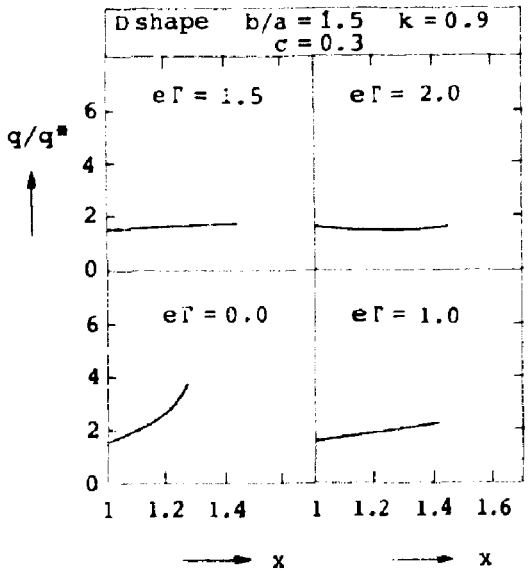

Figs. 7: q-profiles in the FFC region outside a high-beta tokamak plasma with a D-shaped cross-section for various values of Γ (b/a = 1.5, c = .3, e = L/2π = 1.267) and for two values of $\varepsilon\beta_p$: $\varepsilon\beta_p$ = .17 (k = .7) and $\varepsilon\beta_p$ = .392 (k = .9).

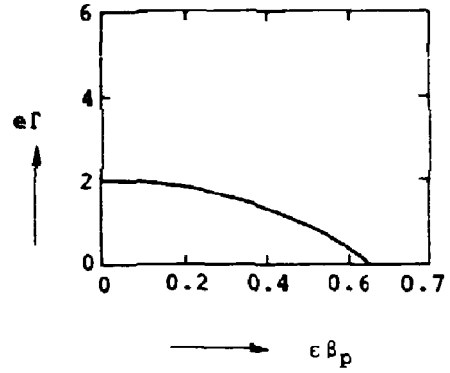

Fig. 8: Relationship between $\bar{\Gamma}$ and $\varepsilon\beta_p$ for a high-beta tokamak plasma with an elliptical cross-section (b/a = 1.5, e = L/2π = 1.262) for which $dq/d\psi\big|_s = 0$.

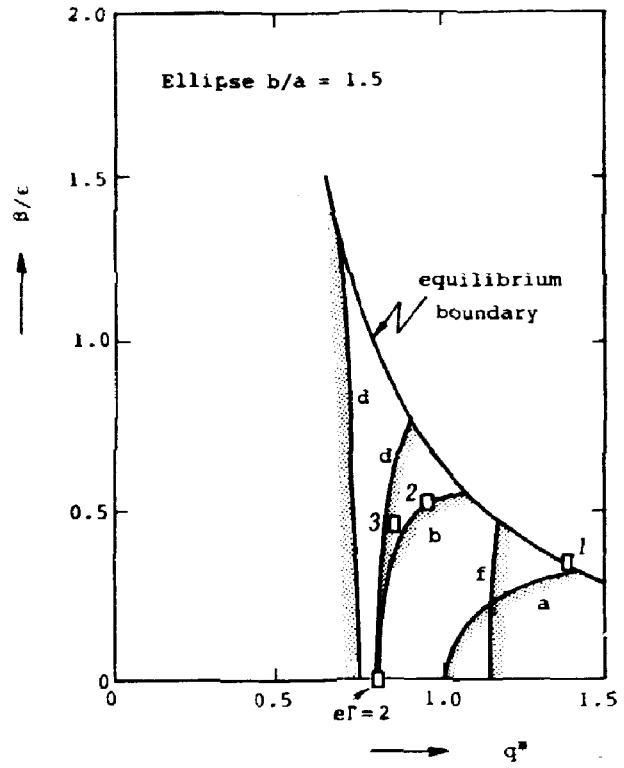

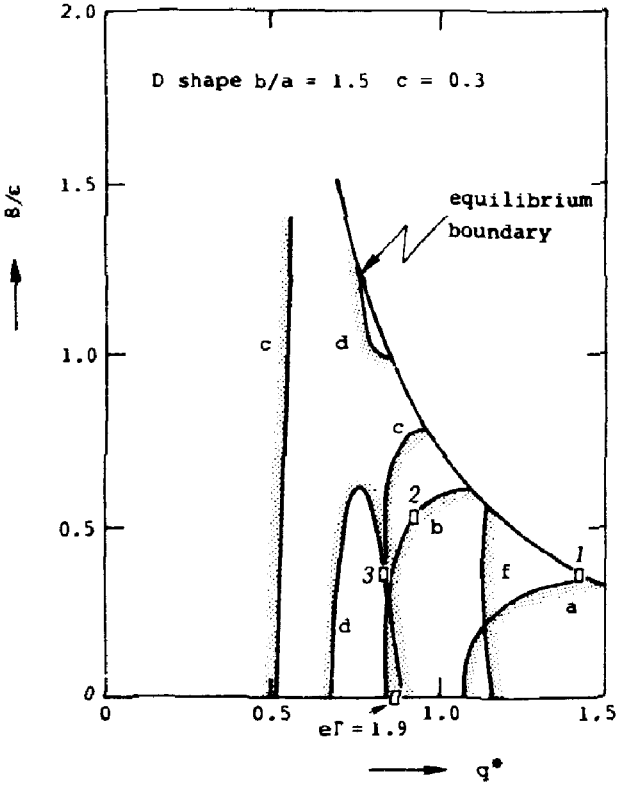

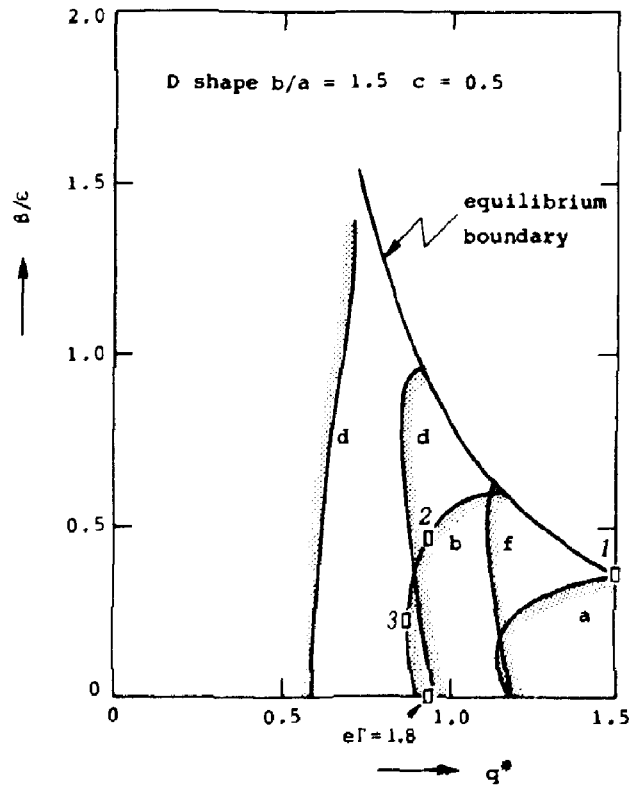

Figs. 9: Marginal stability curves for a high-beta tokamak plasma with different cross-sections and for various values of eΓ: a) eΓ = 0, b) eΓ = 1, c) eΓ = 1.5, d) eΓ = 2, f) eΓ = 3; the shaded side indicates the stable region. The marginal stability points corresponding to the screw-pinch are indicated by ○; the value of eΓ at the points 1,2, 3 is respectively eΓ = .1, 1 and 1.5; the value of e for these cross-sections is: ellipse e = 1.262, D-shape (c = 0.3) e = 1.267, D-shape (c = 0.5) e = 1.273.

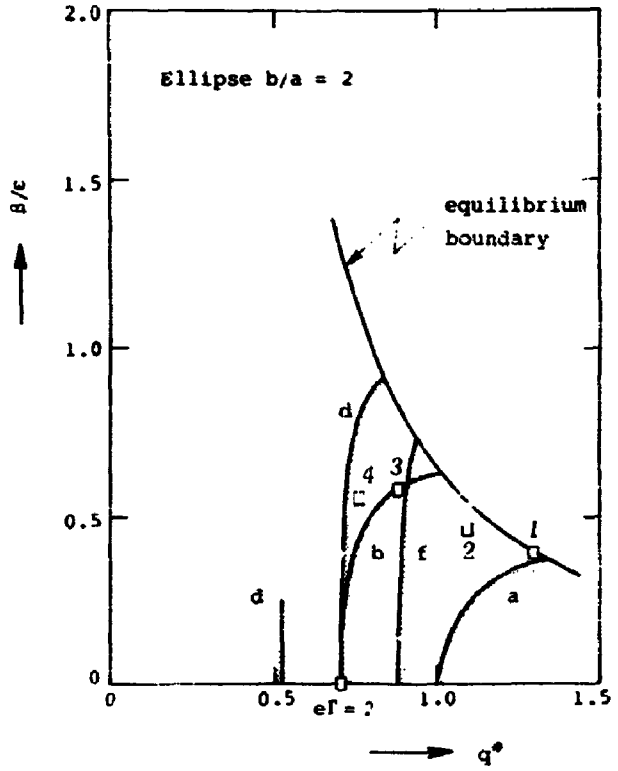

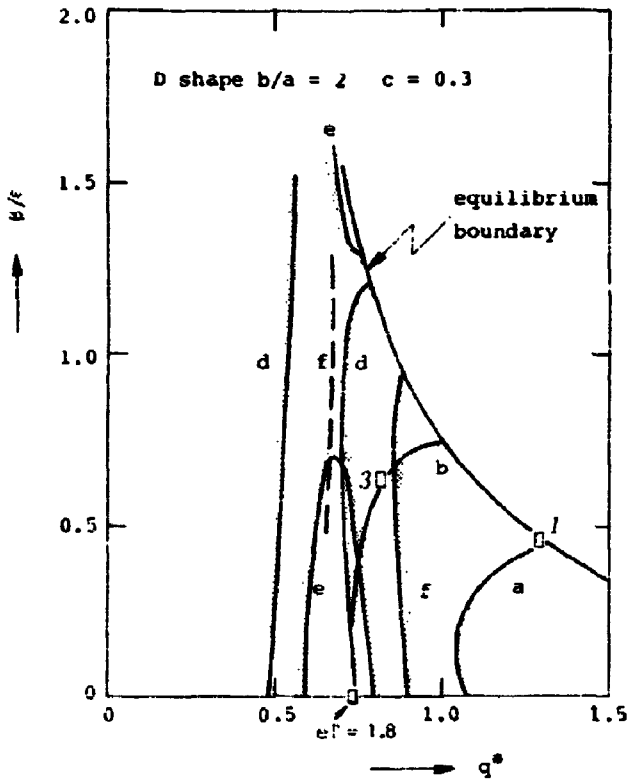

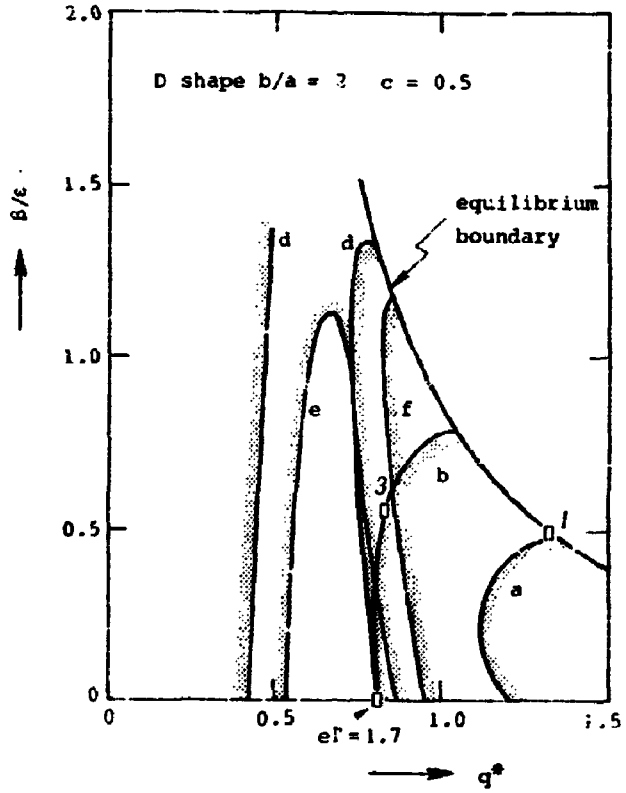

Figs. 10: Marginal stability curves for a high-beta tokamak plasma with different cross-sections and for various values of eΓ: a) eΓ = 0, b) eΓ = 1, d) eΓ = 2, e) eΓ = 2.5, f) eΓ = 3; the shaded side indicates the stable region. The marginal stability points corresponding to the screw-pinch are indicated by ⊔; the value of eΓ at the points 1,2,3,4 is respectively: eΓ = .1, .5, 1 and 1.5; the value of e for these cross-sections is: ellipse e = 1.542, D-shape (c = 0.3) e = 1.545, D-shape (c = 0.5) e = 1.55.

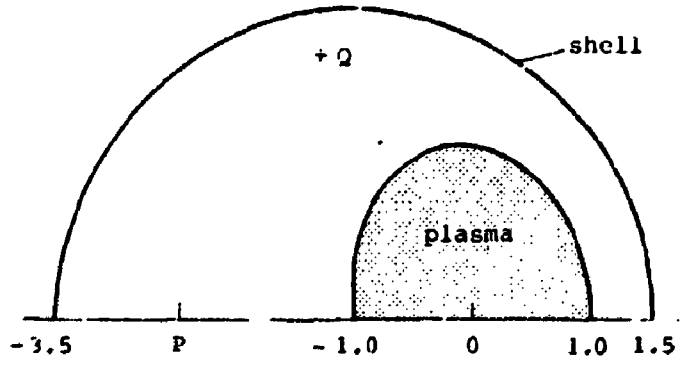

Fig. 11: Equilibrium of a high-beta tokamak plasma with respect to a conducting wall, with a circular cross-section, from a free-boundary analysis ($\varepsilon\beta_p$ = .493 or k = .955).